Laboratory Research
J Korean Neurosurg Soc 67 (3) : 333-344, 2024
https://doi.org/10.3340/jkns.2023.0154
pISSN 2005-3711 eISSN 1598-7876

Prospero Homeobox 1 and Doublecortin Correlate with Neural Damage after Ischemic Stroke

Dong-Hun Lee,[1,*] Eun Chae Lee,[2,*] Sang-Won Park,[1] Ji young Lee,[3] Kee-Pyo Kim,[2] Jae Sang Oh[3]

Department of Neurosurgery,[1] Soonchunhyang University Cheonan Hospital, College of Medicine, Soonchunhyang University, Cheonan, Korea
Department of Medical Life Sciences,[2] College of Medicine, The Catholic University of Korea, Seoul, Korea
Department of Neurosurgery,[3] Uijeongbu St. Mary's Hospital, College of Medicine, The Catholic University of Korea, Seoul, Korea

Objective : Markers of neuroinflammation during ischemic stroke are well characterized, but additional markers of neural damage are lacking. The study identified associations of behavioral disorders after stroke with histologic neural damage and molecular biological change.

Methods : Eight-week-old, 25 g male mice of the C57BL/6J strain were subjected to middle cerebral artery occlusion (MCAO) to induce ischemic stroke. The control group was a healthy wild type (WT), and the experimental group were designed as a low severity MCAO1 and a high severity MCAO2 based on post-stroke neurological scoring. All groups underwent behavioral tests, real-time polymerase chain reaction, triphenyltetrazolium chloride (TTC) staining and Hematoxylin and Eosin staining. One-way analysis of variance was used to analyze statistical significance between groups.

Results : In TTC staining, MCAO1 showed 29.02% and MCAO2 showed 38.94% infarct volume (p<0.0001). The pro-inflammatory cytokine interleukin (IL)-1β was most highly expressed in MCAO2 (WT 0.44 vs. MCAO1 2.69 vs. MCAO2 5.02, p<0.0001). From the distance to target in the Barnes maze test, WT had a distance of 178 cm, MCAO1 had a distance of 276 cm, and MCAO2 had a distance of 1051 (p=0.0015). The latency to target was 13.3 seconds for WT, 27.9 seconds for MCAO1, and 87.9 seconds for MCAO2 (p=0.0007). Prospero homeobox 1 (*Prox1*) was most highly expressed in MCAO2 (p=0.0004). Doublecortin (*Dcx*) was most highly expressed in MCAO2 (p<0.0001).

Conclusion : The study demonstrated that histological damage to neural cells and changes in brain mRNA expression were associated with behavioral impairment after ischemic stroke. *Prox1* and *Dcx* may be biomarkers of neural damage associated with long-term cognitive decline, and increased expression at the mRNA level was consistent with neural damage and long-term cognitive dysfunction.

Key Words : Ischemic stroke · Cerebral infarction · Middle cerebral artery occlusion · Long-term memory.

• Received : July 20, 2023 • Revised : September 28, 2023 • Accepted : October 16, 2023
• Address for reprints : **Kee-Pyo Kim**
Department of Medical Life Sciences, College of Medicine, The Catholic University of Korea, 222 Banpo-daero, Seocho-gu, Seoul 06591, Korea
Tel : +82-2-2258-7224, E-mail : kpkim@catholic.ac.kr, ORCID : https://orcid.org/0000-0002-8666-8444

Jae Sang Oh
Department of Neurosurgery, Uijeongbu St. Mary's Hospital, College of Medicine, The Catholic University of Korea, 271 Cheonbo-ro, Uijeongbu 11765, Korea
Tel : +82-31-820-2024, E-mail : metatron1324@hotmail.com, ORCID : https://orcid.org/0000-0003-4570-6763

*These authors contributed equally to this work.

INTRODUCTION

A stroke is a general term for a sudden, focal neurological deficit caused by an abnormality in blood flow to the brain[18]. An ischemic stroke occurs when the blood supply to a localized area of the brain is reduced, resulting in dysfunction in that area. The central nervous system affected by an ischemic stroke develops aphasia, vision defects, memory deficits, and impaired thinking. When the blood vessels to the brain are compromised, the supply of glucose, the brain's energy source, is compromised[22]. When glucose is the only source of energy, brain tissue is more susceptible to necrosis. This damage to brain tissue caused by abnormalities in cerebral blood flow can lead to symptoms of cognitive impairment. Ischemic stroke triggers an ischemic cascade[5,6]. Ischemic conditions induce the production of oxygen free radicals and reactive oxygen species, which can damage cells[25].

Some patients who have suffered a stroke will have residual disability even after receiving treatment[15,23]. More than half of patients receiving acute therapy progress to long-term disability. With the development of acute therapies, survival rates for stroke patients have improved[8,14,29]; however, post-stroke cognitive impairment and dementia remain prevalent[11,13,19,26,27], with 70% of stroke survivors experiencing cognitive impairment among their sequelae[28].

In ischemic stroke, there are several well-studied biomarkers that can identify neuroinflammation from the ischemic cascade, including interleukin (IL)-1β, IL-6, and tumor necrosis factor[3]. On the other hand, biomarkers for neural damage after ischemic stroke are less well studied. The expression of inflammation-related factors is upregulated in ischemic stroke conditions. However, an increase in inflammatory factors does not necessarily mean that an ischemic stroke will occur. The authors were convinced of the need for a neural damage biomarker that could demonstrate neural damage along with the progression of the ischemic cascade. A study was conducted to find biomarkers of neural damage after ischemic stroke.

MATERIALS AND METHODS

Experimental animal and research design

All experiments were conducted under the approval of IACUC (SCH22-0097). The housing area of the mice used in the experiments was subjected to a 12-hour light/dark cycle (7:00 a.m. to 7:00 p.m.), the room temperature was maintained at 23°C±1°C, and the room humidity was maintained at 50%± 5%.

Experimental animal and classification criteria

The experimental animals used in the study were house mice (*Mus musculus*) supplied by RaonBio (Yongin, Korea). All mice were male, C57BL/6J strain, weighing 25 g and aged 8 weeks, and were randomly assigned to groups. The groups were designed as a healthy wild-type (WT, n=6) control group, a low-severity middle cerebral artery occlusion (MCAO) 1 (n=6) group, and a high-severity MCAO2 (n=6) group based on neurological scoring after ischemic stroke. The classification criteria were based on previous studies that identified the most pronounced neurological impairment at 48 hours after MCAO, so individuals with a 48-hour neurological score of less than 4 were classified as MCAO1, the low-impairment group, and individuals with a score of more than 4 were classified as MCAO2, the high-impairment group.

MCAO surgery

The experimental group performed Longa et al.[20]'s MCAO method to implement a mouse model of sequelae after ischemic stroke. Blood flow was measured by noninvasive laser Doppler (OxyFlo™ Pro; OXFORD OPTRONIX, Banbury, UK) in three phases : before, during, and after, to determine normal blood flow, blood flow during MCAO, and blood flow after achieving reperfusion.

After induction of anesthesia at 2.5%, isoflurane was maintained at 1.5%. The body temperature of the mouse was maintained at 37°C degrees with a heating pad. Mouse MCAO was performed to induce reperfusion after ischemic stroke. After vascular clamping the left common carotid artery (CCA), left internal carotid artery (ICA), and left external carotid artery (ECA) of the mouse, the MCAO filament was inserted through the incision after temporarily ligating the left ECA. Place the MCAO filament past the ICA and into the M1 region of the MCA to achieve occlusion. After 30 minutes of MCAO, the filament was removed to achieve reperfusion, and the incision was sutured. After surgery, the mice were provided with a heat irradiator and a recovery diet.

 https://doi.org/10.3340/jkns.2023.0154

Post-operative care and neurological score

After waking up from anesthesia, the mice were given a recovery diet. Neurological scores were then measured to determine the extent of neural damage of post-ischemic stroke and mouse health. All mice were measured, and two measures were performed : torso turning and forepaw grip strength. Measurements were taken immediately after awakening from anesthesia and on days 1, 2, 3, and 7 after MCAO. The torso rotation test measures the degree to which the mouse's body curves in the air in the direction opposite to the side on which the hemiparesis is induced by grabbing the mouse's tail and lifting it. A score of 3 is given for an immeasurable amount of body flexion, 2 for severe body flexion, 1 for mild body flexion, and 0 for no movement at all. For the forefoot strike test, the athlete is asked to hold the bar with both forefoots, and the point at which the forefoot that induces unilateral paralysis falls before the contralateral forefoot. A score of 3 is given for unmeasurable hemiparesis, 2 for a very fast fall of the hemiparetic forefoot before the contralateral forefoot, 1 for a slow fall of the forefoot with mild hemiparesis, and 0 if both forefoots have no problem gripping the bar. Each score for torso turning and grip strength was added together to give everyone a rating from 0 to a maximum of 6.

Behavioral tests

All groups were subjected to behavioral tests to analyze behavioral changes in activity and cognitive memory due to ischemic stroke. Behavioral analysis began on day 7 after MCAO and lasted for a total of 5 days (day 11 after MCAO), including an adaptation period, in which experiments were designed from low to high external stimuli to account for the continuous stress of the mice. Each behavioral experiment was video recorded for analysis.

Open field test

A cube-shaped transparent acrylic box (x×y×z, 45×45×45 cm) with an open top is divided into a central zone and a peripheral zone corresponding to 50% of the area of the horizontal axis (x) and vertical axis (y), and the mouse is introduced from the central zone and allowed to move freely for 10 minutes. After the end of the experiment, the total distance traveled is analyzed using behavioral analysis software.

Barnes maze test

Designate 18 localized zones in a circular field 92 cm in diameter, with only one of them containing the mouse's usual diet. Divide the field into quadrants, allocating 25% of the field to each. The mice start in the center of the field and have three minutes to explore freely, ending early if they reach the food source before the 3 minutes are up. After 3 days of adaptation, analyze latency and distance to target on the fourth test day.

Adhesive removal test

Attach a single-sided tape (x×y, 3×2 mm) to one forepaw of a mouse and place it in a translucent cage with no bedding to allow it to behave freely. Observe the mouse for up to 2 minutes and analyze the time it takes for the mouse to remove the tape. Measure both forepaws, starting with one side and switching to the other side when finished.

Analyzing camera tracking

During the behavioral experiments, the recorded videos were analyzed with Smart 3.0 Video Tracking System software (Panlab, Barcelona, Spain). Smart 3.0 detects movement by comparing the current video with a reference image. Behavioral differences between each mouse individual were analyzed and quantified by precise automatic measurements of experimental time, mouse position, distance traveled between zones, mouse occupancy time, and the number of times the mouse crossed between zones.

Real time-polymerase chain reaction (RT-PCR)

At the end of the behavioral tests experiment, the group was randomly divided into two groups : one for histological analysis and the other for messenger RNA (mRNA) level analysis.

Brain tissue harvesting

Mice were euthanized by cervical dislocation after induction of isoflurane respiratory anesthesia. After confirmation of euthanasia, the neck was decapitated with surgical scissors to obtain the head separately, the scalp was rolled up to the front of the head to obtain the skull, forceps were inserted subdural and gently lifted outward to remove bone, and whole brain tissue was obtained. The brain tissue was transferred to a microtube, and 1 mL of easy-BLUE (trizol) was added. Immediately, the brain tissue and easy-BLUE were mixed evenly

using a homogenizer.

RNA extraction

Add 200 μL of chloroform to the homogeneously mixed tissue and solution, mix, and run the centrifuge at 13000 rpm, 4°C for 10 minutes. After 10 minutes, when the protein, DNA and RNA layers are separated, take 400 μL from the RNA layer, which is the clear supernatant, transfer it to a 1.5 mL microtube and add equal volume of isopropanol (1 : 1) to precipitate the RNA for 10 minutes. After precipitation, centrifuge again at 13000 rpm, 4°C for 5 minutes. Check the RNA pellet after centrifugation and carefully remove only the supernatant. After removal, add 1 mL of ethanol diluted in 75% nuclease free water (NFW) to wash away the remaining solvent. Centrifuge again at 10000 rpm, 4°C for 5 minutes, remove the supernatant, and dry the pellet until it is dry. Add 20 μL of pre-heated NFW and quantify the amount of RNA via nanodrop at 1000 ng/mL, calibrating all individuals equally.

cDNA synthesis

Add the calibrated RNA dilution to the RNA dilution, NFW, and 2 μL of master mix according to the standard protocol provided by All-In-One 5X cDNA Master Mix (CellScript, Madison, WI, USA) to a final volume of 10 μL. After addition, proceed with cDNA synthesis by reverse transcription according to the standard protocol for cDNA synthesis provided by the T100 Thermal Cycler (BIO-RAD, Contra Costa, CA, USA). Upon completion of synthesis, add 90 μL of NFW to dilute to 1/10.

RT-PCR

In one well of a 96-well plate, dispense 14 μL of primers, SYBR green, and NFW corresponding to the transcripts you want to target according to the standard protocol, then add 1 μL of cDNA for everyone for a total volume of 15 μL. Place a PCR sealing film on top of the 96 wells to prevent the contents of each well from evaporating and foreign substances from entering. Load the plate into the CFX96 Real-Time PCR System (BIO-RAD) and proceed with the polymerase reaction according to the PCR protocol. The PCR protocol is 95°C for 15 minutes, followed by 40 cycles of 95°C for 10 seconds, 60°C for 15 seconds, and 72°C for 20 seconds.

Triphenyltetrazolium chloride (TTC) staining

After euthanizing the mice, follow the same procedure for harvesting brain tissue for RNA extraction before homogenization. Obtain complete brain tissue, embed it in brain matrix, shape it, and cut it with a razor blade to obtain brain tissue sections at 2 mm intervals. The obtained brain tissue sections are completely immersed in a 2% dilution of TTC, wrapped in foil, and incubated in an incubator at 37°C for 30 minutes. After incubation, the unstained area (white) of the total tissue area was measured as a percentage (%) using Image J software (National Institutes of Health, Bethesda, MD, USA).

Hematoxylin and Eosin (H&E) staining

Once the mouse is unconscious under respiratory anesthesia, make an incision between the ribs and abdomen to access the heart. Once visualized, insert the needle into the convex convergence at the tip of the heart to inject phosphate buffered saline (PBS) via syringe. Once the needle is inserted, slowly inject PBS to achieve perfusion. Once perfusion is achieved, the brain is obtained through the same incision and the tissue is fixed by complete immersion in 4% paraformaldehyde. The fixed brain tissue was sectioned to a thickness of approximately 2–3 mm and subjected to tissue processing (STP120 Spin tissue Processor; Especialidades Médicas MYR, S.L., Tarragona, Spain). The processed tissue was sectioned using a sectioning machine (Finesse ME Microtome; Thermo Fisher Scientific, Waltham, MA, USA) to a thickness of approximately 3–4 μm, and the sections were attached to slides for drying, deparaffinized in xylene for 3 steps/3 minutes, hydrated in alcohol for 4 steps/2 minutes, hematoxylin for 10 minutes, water for 3 minutes, eosin for 1 minute 40 seconds, alcohol for 4 steps/1 minute, cleared in xylene for 3 steps/3 minutes, and embedded to prepare H&E sections.

Statistical analysis

Quantitative data obtained through behavioral tests analysis, mRNA level analysis, TTC staining were graphed and statistically analyzed using GraphPad Prism 8 software (GraphPad Software, Boston, MA, USA). Statistically differences between each control and experimental group were tested for significance using one-way analysis of variance.

 https://doi.org/10.3340/jkns.2023.0154

RESULTS

MCAO blocks cerebral blood flow, leading to ischemic stroke

In the MCAO group, reperfusion was performed after Longa MCAO (Fig. 1). Immediately before occlusion of the M1 segment of the middle cerebral artery, blood flow was measured by noninvasive laser doppler, which revealed an average blood flow of 400 blood perfusion unit (BPU). During the MCAO, researcher found 0 BPU, and when researcher achieved filament retraction and blood reperfusion, researcher found blood flow reperfusion between 300 BPU and 400 BPU.

For all groups, brain tissue obtained after sacrifice at the end of the behavioral analysis was subjected to TTC staining for cerebral infarct localization, and cerebral infarction was confirmed in the MCAO1 and MCAO2 groups (Fig. 2A). No cerebral infarction was identified in WT (0%), 29.02%±7.74% in MCAO1 and 38.94%±3.74% in MCAO2, with MCAO2 having the highest infarct volume expression (p<0.0001). MCAO2 showed a higher infarct volume than MCAO1 (p=0.0065). MCAO2 scored higher on neurological scoring measures, confirming the damaged brain (Fig. 2B).

MCAO group expressed neuroinflammatory brain damage due to ischemic cascade

The MCAO group that experienced ischemic stroke had neuroinflammatory damage from the ischemic cascade (Fig. 2D).

RT-PCR performed to determine differences in mRNA level expression showed that the mRNA levels of vascular cell adhesion molecule 1 (*Vcam1*), which contributes to immune cell adhesion[9], were 0.81±0.22 in WT, 1.74±0.21 in MCAO1, and 3.61±0.95 in MCAO2 (p<0.0001). The mRNA level of *Vcam1* in MCAO2 was higher than in MCAO1 (p=0.0013).

The mRNA level of intercellular adhesion molecule 1

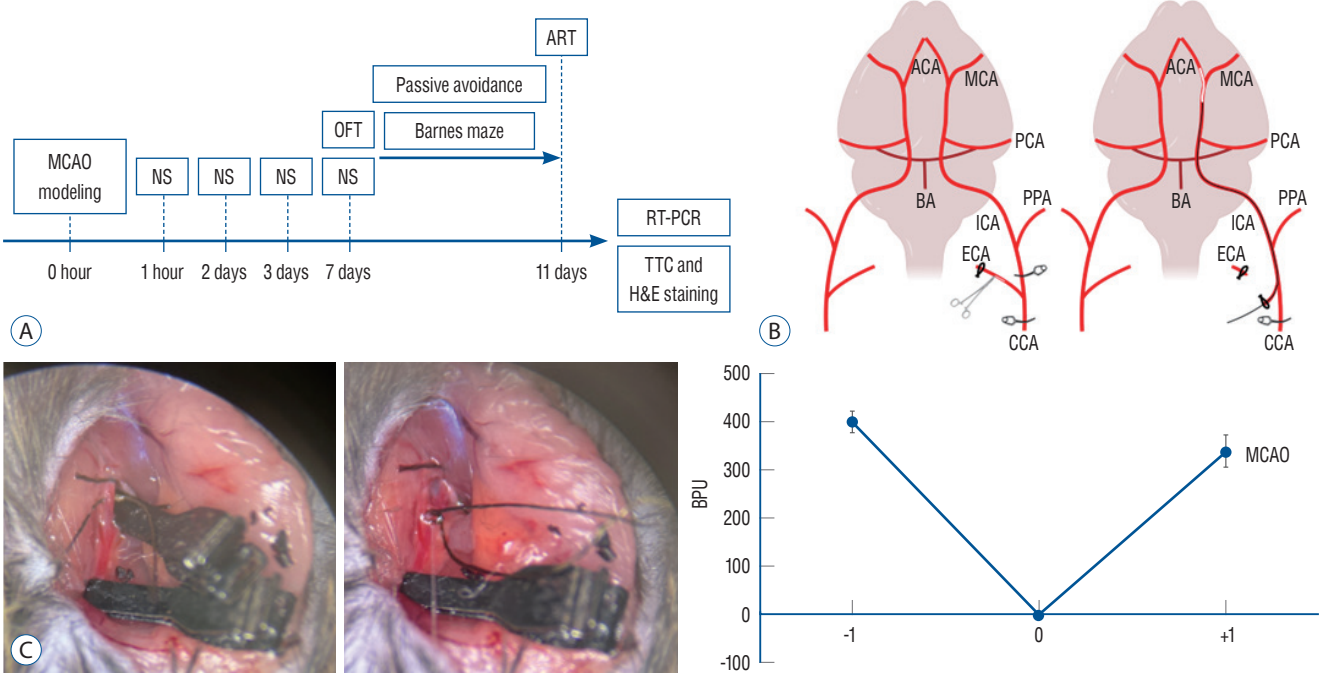

Fig. 1. A : Overview of experimental design in the MCAO mouse model. All MCAO mice are neurologically scored post-operatively and undergo behavioral experiments sequentially from low to high stress starting on day 7. Upon completion of the behavioral experiments, brain tissue is harvested by euthanasia and sampled for mRNA level expression and histological staining. B : MCAO surgery to induce ischemic stroke in mice. Blood flow to the CCA, ICA, and ECA is blocked via a vascular clamp, and then an MCAO suture is inserted through an incision in the ECA to achieve M1 site occlusion. C : Advancing a filament through an ECA incision in a mouse to the MCA. Immediately before middle cerebral artery occlusion (x-axis of the graph : -1), blood flow in the middle cerebral artery averaged 400 BPU, and during occlusion, it was 0 BPU. After reperfusion, blood flow ranged from 300 BPU to 400 BPU, depending on the individual, confirming that reperfusion was achieved. MCAO : middle cerebral artery occlusion, NS : neurological score, OFT : open field test, ART : adhesive removal test, RT-PCR : real-time polymerase chain reaction, TTC : triphenyltetrazolium chloride, H&E : Hematoxylin and Eosin, ACA : anterior cerebral artery, MCA : middle cerebral arte, PCA : posterior cerebral artery, BA : basilar artery, ICA : internal carotid artery, PPA : pterygopalatine artery, ECA : external carotid artery, CCA : common carotid artery, BPU : blood perfusion units.

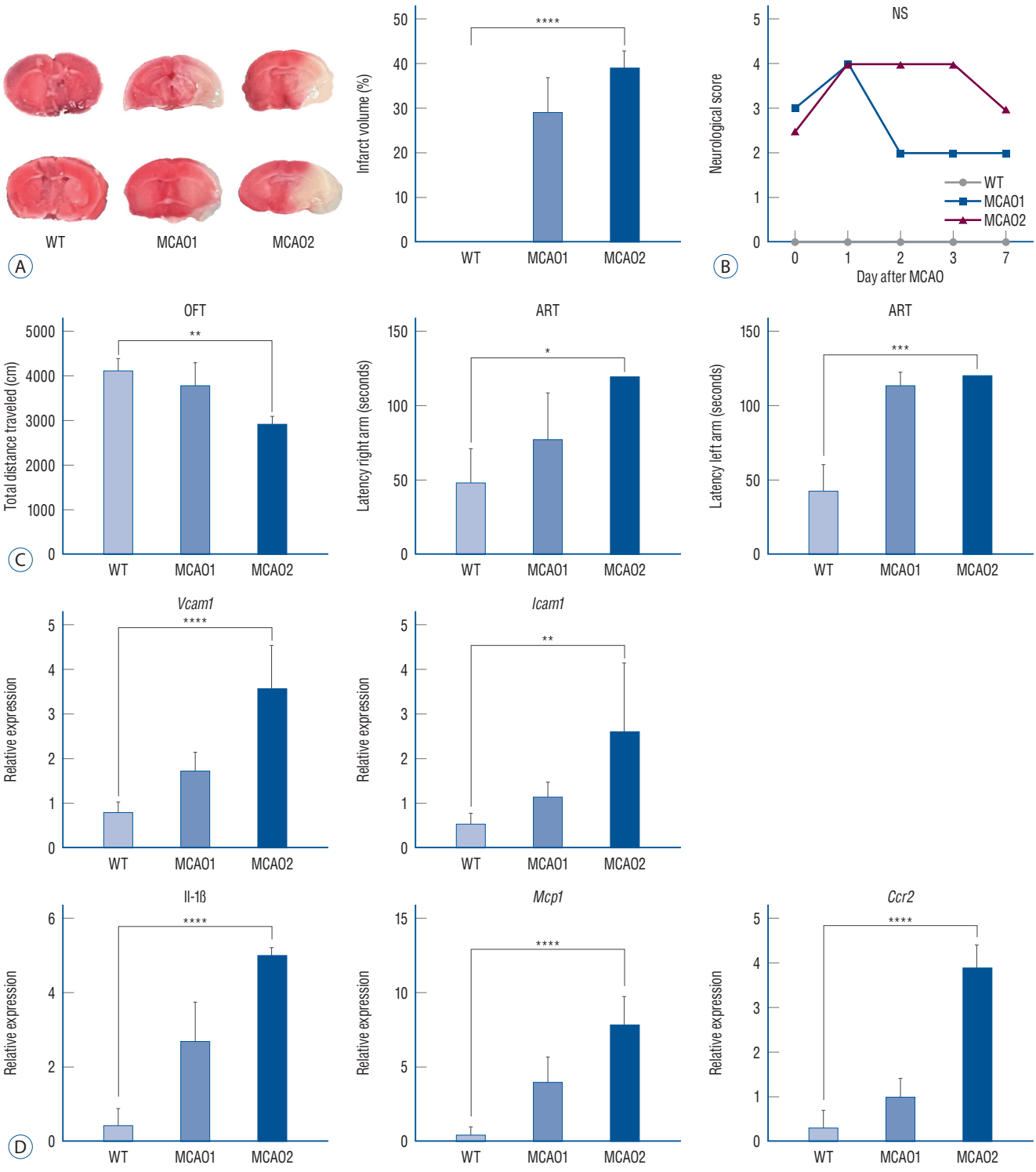

Fig. 2. A : Measurement of brain infarct volume and neurological scores in the MCAO group. TTC staining in WT, MCAO1, and MCAO2 groups. Measurement of infarct volume in MCAO1 and MCAO2. B : Measurement of neurological scores after MCAO. C : Locomotor activity and sensorimotor changes in the MCAO group. Measured the total distance traveled in the open field test and the adhesive removal latency of ART for the WT and MCAO groups. D : Neuroinflammation-related mRNA levels in the MCAO group. *p<0.05, **p<0.01, ***p<0.001, ****p<0.0001. WT : wild type, MCAO : middle cerebral artery occlusion, NS : neurological score, OFT : open field test, ART : adhesive removal test, *Vcam1* : vascular cell adhesion molecule 1, *Icam1* : intercellular adhesion molecule 1, IL : interleukin, *Mcp1* : monocyte chemoattractant protein 1, *Ccr2* : C-C chemokine receptor 2, TTC : triphenyltetrazolium chloride.

 https://doi.org/10.3340/jkns.2023.0154

(*Icam1*), which contributes to immune cell adhesion[9], showed expression levels of 0.54±0.24 in WT, 1.15±0.33 in MCAO1, and 2.63±1.53 in MCAO2 (p=0.0037). The mRNA level of *Icam1* in MCAO2 was higher than in MCAO1 (p=0.0423).

The mRNA level of the pro-inflammatory cytokine[17] IL-1β was 0.44±0.44 in WT, 2.69±1.06 in MCAO1, and 5.02±0.20 in MCAO2 (p<0.0001). The mRNA level of IL-1β in MCAO2 was higher than in MCAO1 (p=0.0004).

The mRNA level of monocyte chemoattractant protein 1 (*Mcp1*), a chemokine receptor that recruits monocytes to the site of inflammation[4], showed expression levels of 0.48±0.50 in WT, 3.98±1.72 in MCAO1, and 7.86±1.85 in MCAO2 (p<0.0001). The mRNA level of *Mcp1* in MCAO2 was higher than in MCAO1 (p=0.0038).

The mRNA level of C-C chemokine receptor 2 (*Ccr2*), which is involved in monocyte infiltration in inflammatory diseases, showed expression levels of 0.33±0.37 in WT, 1.02±0.39 in MCAO1, and 3.89±0.51 in MCAO2 (p<0.0001). The mRNA level of *Ccr2* in MCAO2 was higher than in MCAO1 (p=0.0001).

Locomotor activity and sensorimotor changes in MCAO

The MCAO group exhibited symptoms of locomotor activity disorders (Fig. 2C). In terms of total distance traveled (cm) in the open field test, WT showed a total distance of 4102±621

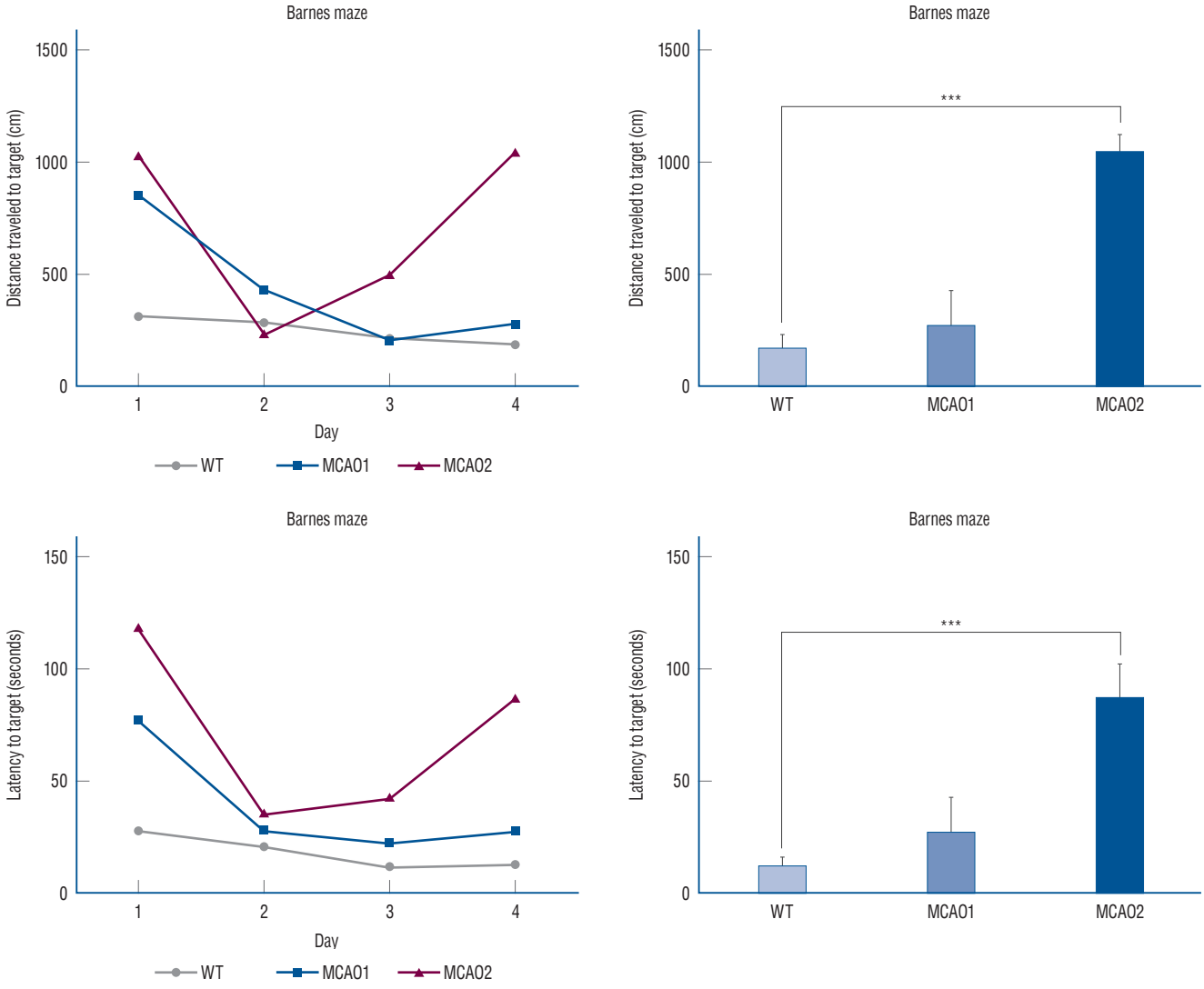

Fig. 3. Measuring positive long-term cognitive memory in the MCAO group. ***p<0.001. WT : wild type, MCAO : middle cerebral artery occlusion.

cm, MCAO1 showed a total distance of 3771±490 cm, and MCAO2 showed a total distance of 2908±188 cm (p=0.0015). The total distance of MCAO2 was lower than MCAO1 (p=0.0024).

In the adhesive removal test for sensorimotor measures, WT showed a latency of 49±23 seconds, MCAO1 88±45 seconds, and MCAO2 120±0 seconds in the right forepaw latency region (latency right arm) (p=0.0168). Right forepaw adhesive removal latency was longer in MCAO2 than in WT (p=0.0055).

In the left forepaw latency measure (latency left arm), WT showed a latency of 43±17 seconds, MCAO1 114±9 seconds, and MCAO2 120±0 seconds (p=0.0004). There was a statistically different. Left forepaw adhesive removal latency was longer in MCAO2 than in WT (p=0.0011).

MCAO expressed impairment in positive long-term cognitive memory

The MCAO group exhibited long-term cognition memory impairment (Fig. 3). In the distance to target (cm), WT had 178±131 cm, MCAO1 had 276±216 cm, and MCAO2 had 1051 ±102 cm (p=0.0004). In distance to target, MCAO2 traveled a longer distance than MCAO1 (p=0.0442).

In the latency to target (seconds), WT showed a latency of 13.3±7.5 seconds, MCAO1 showed a latency of 27.9±21.1 seconds, and MCAO2 showed a latency of 87.9±21.2 seconds (p=0.0007). MCAO2 showed longer latency than WT in latency to target (p=0.0002).

Altered mRNA levels of prospero homeobox 1 (*Prox1*) and Doublecortin (*Dcx*) and neural damage in MCAO

The MCAO group had confirmed neural cell damage (Fig. 4A). In healthy WT, neural cell arrangement was even, and no apoptosis was identified, MCAO1 had no apoptosis but hippocampal arrangement atrophy was identified, and MCAO2 had extensive apoptosis.

The mRNA level of *Prox1*, a marker of early hippocampal development[12], was found to be higher in MCAO2 than MCAO1 (Fig. 4B). WT had mRNA levels of 1.12±0.46, MCAO1 had 2.03±0.64, and MCAO2 had 3.36±1.01 (p=0.0004).

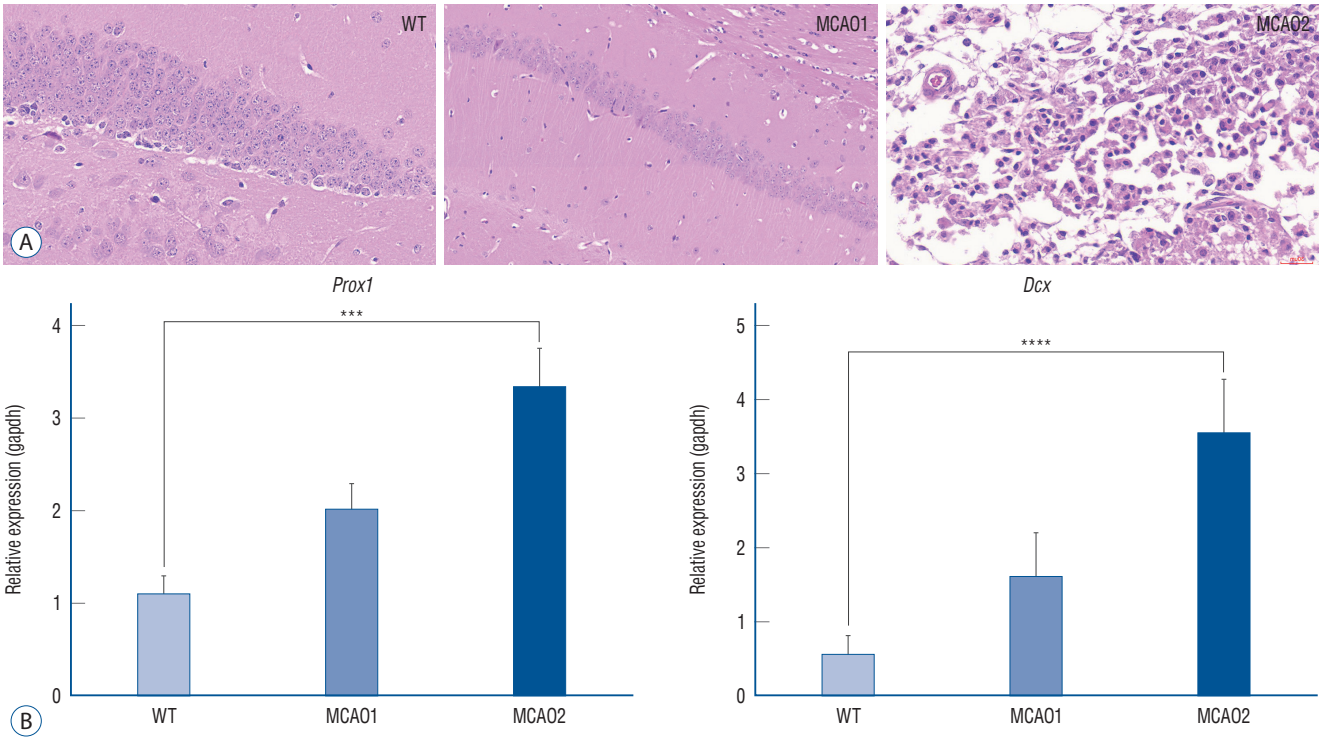

Fig. 4. Histological finding in hippocampus and neural biomarker mRNA levels in the MCAO group. A : Hematoxylin and Eosin (H&E) staining of two groups of WT and MCAO. Microscopy showing cellular arrangement and apoptosis in the hippocampal region with H&E staining (×350). B : mRNA levels of *Prox1* and *Dcx* in WT and MCAO groups. ***p<0.001, ****p<0.0001. WT : wild type, MCAO : middle cerebral artery occlusion, *Prox1* : prospero homeobox 1, *Dcx* : doublecortin.

 https://doi.org/10.3340/jkns.2023.0154

The mRNA expression level of *Prox1* was higher in MCAO2 than in MCAO1 (p=0.0215).

The mRNA level of *Dcx*, a neuroregeneration marker[24], was found to be higher in MCAO2 than MCAO1 (Fig. 4B). WT had mRNA levels of 0.59±0.24, MCAO1 had 1.63±0.58, and MCAO2 had 3.57±0.71 (p<0.0001). The mRNA expression level of *Dcx* was higher in MCAO2 than in MCAO1 (p=0.0004).

DISCUSSION

Increased mRNA level expression of *Prox1* and *Dcx* may be a marker of neuronal damage (Fig. 5). Among the behavioral disorders after ischemic stroke, impairment of long-term cognitive memory is present. The formation of memories involves the Papez circuit and the limbic system[1,31]. Explicit memories are conscious, intentional memories that are generated by information and experiences[30]. The hippocampus, amygdala, striatum, and others are involved in motivation, emotion, learning, and memory. Damage to the hippocampus can affect spatial memory and cognition in general[7]. *Prox1* is expressed in the early hippocampus[10]. The expression of *Prox1* in the severe MCAO2 group was the highest compared to the MCAO1 group, and tissue H&E staining to identify neural damage confirmed brain tissue damage, with consistent results in the Barnes maze test. It is hoped that *Prox1* and *Dcx* can be utilized as a novel predictor of neural damage. *Prox1* is specifically expressed in the dentate gyrus[16], which is part of the hippocampal synaptic circuitry, and contributes to the formation of new memories and spontaneous exploration[10]. The authors found that *Prox1* has higher mRNA expression in higher levels of neural damage, which is associated with worse long-term cognitive function. This study found that MCAO2 with higher severity had the highest mRNA expression levels of *Prox1*. Consistent with H&E staining confirming hippocampal apoptosis in the MCAO group, it predicts that the in-

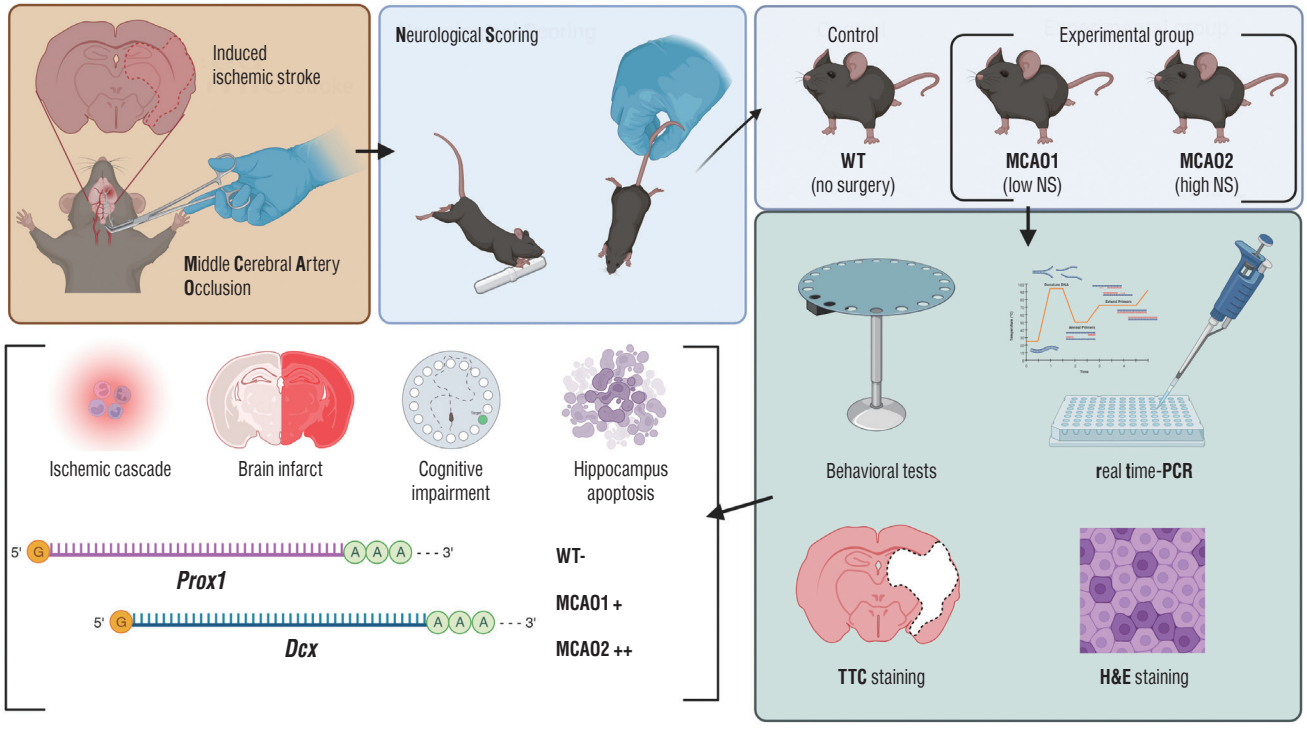

Fig. 5. Overview of experiments to identify behavioral, histological, and molecular biological changes induced by neural damage after ischemic stroke. Created a mouse model that mimics human ischemic stroke by inducing MCAO through surgical intervention. The mice were then evaluated for NS and categorized into low or high symptom groups based on the severity of their symptoms. The groups were then assessed for the impact of ischemic stroke through behavioral and histological analysis. At the end of the analysis, conclusions were drawn about two genes, *Prox1* and *Dcx*. WT : wild type, MCAO : middle cerebral artery occlusion, NS : neurological score, *Prox1* : prospero homeobox 1, *Dcx* : doublecortin, PCR : polymerase chain reaction, TTC : triphenyltetrazolium chloride, H&E : Hematoxylin and Eosin.

creased mRNA level expression of *Prox1* is an early hippocampal marker and is expressed by hippocampal damage. *Dcx* is a protein expressed in neural progenitor cells and immature neurons. In healthy adult neurons, downregulation of *Dcx* is observed along with the expression of neuronal nuclear[2]. The *Dcx* is a neurogenesis marker, which is increased in cerebral ischemia[21]. When this research compared the extent of neural damage in high-severity MCAO2 and low-severity MCAO1 by tissue staining, it found lower expression of *Prox1* and *Dcx*, consistent with lower neural damage in MCAO1.

Elevated mRNA expression levels of *Prox1* and *Dcx* were associated with deterioration of locomotor activity and upregulation of neuroinflammation-related biomarkers. TTC staining was used to measure brain infarct volume in the MCAO groups, and the MCAO2 group, which had the highest severity of neural damage, had the highest brain infarct volume. The expression of symptoms of cerebral infarction and hemiplegic disorders appears to be caused by cerebral ischemic damage by the ischemic cascade after stroke, which is the same in human ischemic stroke. The lack of oxygen and energy supply due to ischemia leads to mitochondrial death and apoptosis. *Vcam1* and *Icam1*, adhesion molecules that help monocytes migrate, were found to be upregulated in the MCAO2 group. Higher mRNA levels of IL-1β, *Mcp1*, and *Ccr2*, inflammation-associated chemokines and cytokines, were found in the MCAO2 group. Behavioral tests confirmed behavioral impairment in the MCAO group. In the open field test, the MCAO2 group showed less activity than the MCAO1 group. In the adhesive removal test, the MCAO2 group had more difficulty removing the tape from both forepaws and reached a delayed maximum time compared to the MCAO1 group. The differences were even more pronounced in the Barnes maze test, which checks for positive long-term cognitive memory. From the first day of preliminary trials, the MCAO2 group spent more distance traveled and latency to reach the destination than MCAO1, and on the day of the final analysis measurements, they experienced many errors, which increased the distance traveled and latency.

There are limitations to the study. While this research has identified mRNA level expression differences to identify ischemic cascades and neural damage, this research lack confirmation that there are differences in regional expression in the form of functioning proteins or cells. It would be an interesting follow-up study to apply ischemic stroke countermeasures, such as thrombolytic or vasodilator drugs, or surgical treatment to the animal models in this study to see if mRNA expression of *Prox1* and *Dcx* is reduced, and cognitive function is restored.

CONCLUSION

The severity of behavioral disorders following ischemic stroke was correlated with the severity of histological damage in the brain and upregulation of biomarkers. Increased mRNA level expression of *Prox1* and *Dcx* is proportional to the severity of neural damage after stroke. This study suggests *Prox1* and *Dcx* as biomarkers of neural damage.

AUTHORS' DECLARATION

Conflicts of interest

No potential conflict of interest relevant to this article was reported.

Informed consent

This type of study does not require informed consent.

Author contributions

Conceptualization : JSO; Data curation : KPK; Formal analysis : DHL, ECL; Funding acquisition : JSO; Methodology : DHL, JSO; Project administration : JSO; Visualization : SWP, JYL; Writing - original draft : DHL, ECL; Writing - review & editing : JSO

Data sharing

None

Preprint

None

ORCID

Dong-Hun Lee https://orcid.org/0000-0003-2629-5225
Eun Chae Lee https://orcid.org/0000-0002-3337-459X
Sang-Won Park https://orcid.org/0000-0001-6304-2126

 https://doi.org/10.3340/jkns.2023.0154

Ji young Lee https://orcid.org/0000-0002-4539-7158
Kee-Pyo Kim https://orcid.org/0000-0002-8666-8444
Jae Sang Oh https://orcid.org/0000-0003-4570-6763

• Acknowledgements

This research was supported by the Bio & Medical Technology Development Program of the National Research Foundation funded by the Korean government (2023RA1A2C100531), by the Korea Medical Device Development Fund grant funded by the Korea government (the Ministry of Science and ICT, the Ministry of Trade, Industry and Energy, the Ministry of Health & Welfare, Republic of Korea, the Ministry of Food and Drug Safety) (HC22C0043). The author(s) wish(es) to ac - knowledge the f inancial support of The Catholic University of Korea Uijeongbu St. Mary's Hospital Clinical Research Laboratory Foundation made in the program year of 2023.

References

1. Aggleton JP, Pralus A, Nelson AJ, Hornberger M : Thalamic pathology and memory loss in early Alzheimer's disease: moving the focus from the medial temporal lobe to Papez circuit. **Brain 139(Pt 7) :** 1877-1890, 2016
2. Brown JP, Couillard-Després S, Cooper-Kuhn CM, Winkler J, Aigner L, Kuhn HG : Transient expression of doublecortin during adult neurogenesis. **J Comp Neurol 467 :** 1-10, 2003
3. Bustamante A, Simats A, Vilar-Bergua A, García-Berrocoso T, Montaner J : Blood/brain biomarkers of inflammation after stroke and their association with outcome: from C-reactive protein to damage-associated molecular patterns. **Neurotherapeutics 13 :** 671-684, 2016
4. Carr MW, Roth SJ, Luther E, Rose SS, Springer TA : Monocyte chemoattractant protein 1 acts as a T-lymphocyte chemoattractant. **Proc Natl Acad Sci U S A 91 :** 3652-3656, 1994
5. Cramer SC : Repairing the human brain after stroke: I. Mechanisms of spontaneous recovery. **Ann Neurol 63 :** 272-287, 2008
6. Deb P, Sharma S, Hassan KM : Pathophysiologic mechanisms of acute ischemic stroke: an overview with emphasis on therapeutic significance beyond thrombolysis. **Pathophysiology 17 :** 197-218, 2010
7. Eichenbaum H : A cortical-hippocampal system for declarative memory. **Nat Rev Neurosci 1 :** 41-50, 2000
8. Goyal M, Menon BK, van Zwam WH, Dippel DW, Mitchell PJ, Demchuk AM, et al. : Endovascular thrombectomy after large-vessel ischaemic stroke: a meta-analysis of individual patient data from five randomised trials. **Lancet 387 :** 1723-1731, 2016
9. Huo Y, Ley K : Adhesion molecules and atherogenesis. **Acta Physiol Scand 173 :** 35-43, 2001
10. Iwano T, Masuda A, Kiyonari H, Enomoto H, Matsuzaki F : Prox1 postmitotically defines dentate gyrus cells by specifying granule cell identity over CA3 pyramidal cell fate in the hippocampus. **Development 139 :** 3051-3062, 2012
11. Jokinen H, Melkas S, Ylikoski R, Pohjasvaara T, Kaste M, Erkinjuntti T, et al. : Post-stroke cognitive impairment is common even after successful clinical recovery. **Eur J Neurol 22 :** 1288-1294, 2015
12. Karalay O, Doberauer K, Vadodaria KC, Knobloch M, Berti L, Miquelajauregui A, et al. : Prospero-related homeobox 1 gene (Prox1) is regulated by canonical Wnt signaling and has a stage-specific role in adult hippocampal neurogenesis. **Proc Natl Acad Sci U S A 108 :** 5807-5812, 2011
13. Koton S, Pike JR, Johansen M, Knopman DS, Lakshminarayan K, Mosley T, et al. : Association of ischemic stroke incidence, severity, and recurrence with dementia in the atherosclerosis risk in communities cohort study. **JAMA Neurol 79 :** 271-280, 2022
14. Lackland DT, Roccella EJ, Deutsch AF, Fornage M, George MG, Howard G, et al. : Factors influencing the decline in stroke mortality: a statement from the American Heart Association/American Stroke Association. **Stroke 45 :** 315-353, 2014
15. Langhorne P, Coupar F, Pollock A : Motor recovery after stroke: a systematic review. **Lancet Neurol 8 :** 741-754, 2009
16. Lavado A, Lagutin OV, Chow LM, Baker SJ, Oliver G : Prox1 is required for granule cell maturation and intermediate progenitor maintenance during brain neurogenesis. **PLoS Biol 8 :** e1000460, 2010
17. Liu T, McDonnell PC, Young PR, White RF, Siren AL, Hallenbeck JM, et al. : Interleukin-1 beta mRNA expression in ischemic rat cortex. **Stroke 24 :** 1746-1750; discussion 1750-1751, 1993
18. Lo EH, Dalkara T, Moskowitz MA : Mechanisms, challenges and opportunities in stroke. **Nat Rev Neurosci 4 :** 399-415, 2003
19. Lo JW, Crawford JD, Desmond DW, Godefroy O, Jokinen H, Mahinrad S, et al. : Profile of and risk factors for poststroke cognitive impairment in diverse ethnoregional groups. **Neurology 93 :** e2257-e2271, 2019
20. Longa EZ, Weinstein PR, Carlson S, Cummins R : Reversible middle cerebral artery occlusion without craniectomy in rats. **Stroke 20 :** 84-91, 1989
21. Lv ZM, Zhao RJ, Zhi XS, Huang Y, Chen JY, Song NN, et al. : Expression of DCX and transcription factor profiling in photothrombosis-induced focal ischemia in mice. **Front Cell Neurosci 12 :** 455, 2018
22. Mergenthaler P, Lindauer U, Dienel GA, Meisel A : Sugar for the brain: the role of glucose in physiological and pathological brain function. **Trends Neurosci 36 :** 587-597, 2013
23. Murray CJ, Vos T, Lozano R, Naghavi M, Flaxman AD, Michaud C, et al. : Disability-adjusted life years (DALYs) for 291 diseases and injuries in 21 regions, 1990-2010: a systematic analysis for the Global Burden of Disease Study 2010. **Lancet 380 :** 2197-2223, 2012
24. Nawabi H, Belin S, Cartoni R, Williams PR, Wang C, Latremolière A, et al. : Doublecortin-like kinases promote neuronal survival and induce growth cone reformation via distinct mechanisms. **Neuron 88 :** 704-719, 2015

25. Olmez I, Ozyurt H : Reactive oxygen species and ischemic cerebrovascular disease. **Neurochem Int 60 :** 208-212, 2012
26. Pendlebury ST, Rothwell PM : Prevalence, incidence, and factors associated with pre-stroke and post-stroke dementia: a systematic review and meta-analysis. **Lancet Neurol 8 :** 1006-1018, 2009
27. Pendlebury ST, Rothwell PM; Oxford Vascular Study : Incidence and prevalence of dementia associated with transient ischaemic attack and stroke: analysis of the population-based Oxford Vascular Study. **Lancet Neurol 18 :** 248-258, 2019
28. Rost NS, Brodtmann A, Pase MP, van Veluw SJ, Biffi A, Duering M, et al. : Post-stroke cognitive impairment and dementia. **Circ Res 130 :** 1252-1271, 2022
29. Toyoda K, Yoshimura S, Nakai M, Koga M, Sasahara Y, Sonoda K, et al. : Twenty-year change in severity and outcome of ischemic and hemorrhagic strokes. **JAMA Neurol 79 :** 61-69, 2022
30. Ullman MT : Contributions of memory circuits to language: the declarative/procedural model. **Cognition 92 :** 231-270, 2004
31. Zarei M, Patenaude B, Damoiseaux J, Morgese C, Smith S, Matthews PM, et al. : Combining shape and connectivity analysis: an MRI study of thalamic degeneration in Alzheimer's disease. **Neuroimage 49 :** 1-8, 2010

 https://doi.org/10.3340/jkns.2023.0154